Beni-Suef University Journal of Basic and Applied Sciences

RESEARCH

Open Access

Entropy generation analysis for magnetohydrodynamic flow of chemically reactive fluid due to an accelerated plate

T. N. Abdelhameed[1,2*]

Abstract

Background The mixed convection flow of viscous fluid due to an oscillating plate is inspected. The external heating effects and chemical reaction assessment are predicted. Moreover, the flow applications of the entropy generation phenomenon are claimed.

Results The dimensionless system is expressed in partial differential forms, which are analytically treated with the Laplace scheme. The physical aspects of the flow model are graphically observed. The optimized phenomenon is focused on flow parameters. The results for the Bejan number are also presented. The dynamic of heat transfer and entropy generation phenomenon is observed with applications of Bejan number.

Conclusions It is claimed that an enhancement of entropy generation phenomenon is noticed due to heat and mass Grashof coefficients. The Bejan number declined due to mass Grashof number. Furthermore, the velocity profile boosted due to Grashof constant.

Keywords Entropy generation, External heat source, Chemical reaction, Bejan number, Laplace technique

1 Background

The mixed convection phenomenon is associated with the fluid flow subject to interaction of forced convection and natural convection. The forced convection is endorsed by external force, while buoyancy forces are subject to the natural convective flow. The role of mixed convection is commonly noted in the different fluid systems as well as industrial processes. A novel role of this phenomenon is also attributed to engineering problems. Basak et al. [1] examined the evaluation in heating phenomenon based on cavity flow with mixed convection effects. Khanafer and Aithal [2] executed analysis for the cylinder flow via significance of mixed convection contribution. Huang et al. [3] explored the mixed convection analysis with convergent channel. Maughan et al. [4] attributed the experimental approach for suggesting the expression for mixed convection in inclined channel. Ahmed et al. [5] suggested the double-driven flow of metallic particles under the mixed convection features. A numerical treatment toward the mixed convention approach was proceeded by Rehman et al. [6]. Hayat et al. [7] intended the optimized aspects of mixed convection problem with Soret features. Sharma et al. [8] elaborated the chemical reaction species for mixed convection flow in inclined surface. Chen et al. [9] suggested the inclined surface flow subject to mixed convection analysis. Ige et al. [10] investigated the transient flow with blood liquid additional forced by mixed convection consequences.

The transport for heat fluctuation phenomenon is important in dynamical systems, engineering mechanisms and thermal devices. The fluctuated impact of thermal generation is preserved for diverse change in

*Correspondence:
T. N. Abdelhameed
t.ahmed@mu.edu.sa
[1] Basic Engineering Sciences Department, College of Engineering, Majmaah University, 11952 Majmaah, Saudi Arabia
[2] Mathematics Department, Faculty of Science, Beni-Suef University, Beni-Suef 62514, Egypt

heat transfer. The heat transfer subject to various flow configurations has been performed in recent years. For instance, Saeed et al. [11] developed a fractional model for Oldroyd-B fluid with heat transfer impact. The analysis was subject to the ramped thermal constraints. Rehman et al. [12] performed heat transfer analysis for second-grade fluid via fractional approach. Saeed et al. [13] observed thermal flow due to chemically reactive Casson fluid with extended boundary constraints. The fractional investigation for heat transfer problem due to Oldroyd-B fluid in view of ramped thermal constraints was analyzed by Saeed et al. [11].

It is commonly observed that for thermal phenomenon, the optimized assessment becomes prime objective to control the loss of heat transfer. Novel role regarding the entropy production is proceeded in the thermal era. For maintaining the fundamental and desirable thermal achievements in electronic systems, sustainability of heat cannot be neglected. The theory of thermodynamics helps in observing the thermal impact for designing various engineering devices and extrusion framework. The first thermodynamics approach conveys the zero energy loss against the transmission of energy. However, this concept is totally unable to predict the fundamental of energy production. The loss and control of thermal energy can be effectively controlled via second thermodynamics approach. The dynamic of entropy production is significantly attributed in the nuclear progress, thermal devices, chemical engineering, extrusion processes, etc. Bejan [14] taken the initiative role for entropy generation by providing the fundamental concept. Li et al. [15] determined the entropy outcomes for porous medium flow with interaction of nanoparticles. Abdelhameed [16] provided the analyzation of entropy generation with sodium alginate material. Shah et al. [17] described the swirling flow under the optimized analysis due to boosted heat transfer. Wang et al. [18] predicted the autocatalysis mechanism based on entropy generation of viscous liquid. Alsallami et al. [19] discussed the rotatory transport with entropy profile via disk flow. Turkyilmazoglu [20] attributed the slip effects with entropy outcomes in channel surface. Batool et al. [21] determined the bioconvective analyzation under optimized impact. Liu et al. [22] identified the grooved flow with contributing the entropy production analysis. The square cavity flow with distribution of entropy judgment was provided by Iftikhar et al. [23]. Sheikholeslami [24] investigated the Lorentz force aspects for entropy generation analysis in porous media. In another work, Sheikholeslami [25] addressed the optimized mechanisms in nanofluid by using the aluminum particles. Sheikholeslami [26–28] presented applications of entropy generation with nanofluid. Abdelhameed [16] addressed the entropy generation of MHD flow of sodium alginate ($C_6H_9NAO_7$) fluid in thermal engineering.

In the above-mentioned literature survey, it is observed that different investigations are inspected for heat and mass transfer phenomenon. The objective of current work is to discuss the mixed convection flow of viscous fluid with assessment of entropy generation phenomenon. The flow observations are supported with the impact of chemically reactive species and external heating source. The Bejan number association with variation of flow parameters is predicted. The solution procedure via Laplace transform is performed. The motivations for performing the current work are to control the loss of heat transfer which is essential in various heat and fluid problems. The simulated results convey applications in thermal systems, solar collectors, heat and fluid problems, chemical engineering, electronic equipment, heat control systems, etc.

2 Methods

2.1 Statement of the problem

Let us assume the mixed convection fluid flow due to the oscillating plate is investigated. The flow pattern is unsteady for moving plates. A static behavior of fluid with adjusted plate is noted with surface uniform temperature θ_∞ and concentration C_∞. The flow configuration is presented in Fig. 1. The deformation in plate at time $\tau = 0^+$ is noted to be $u(0,\tau) = A\tau^2$. The fluctuation in temperature as well as concentration is assumed to be $\theta(y,0) = \theta_\infty$ to $\theta(0,\tau) = \theta_w$,$C(y,0) = C_\infty$, $C(0,\tau) = C_w$, respectively.

The flow equations are [9, 16]:

$$\rho\frac{\partial u(y,\tau)}{\partial \tau} = \mu\frac{\partial^2 u(y,\tau)}{\partial y^2} + \rho g\beta_\theta(\theta(y,\tau) - \theta_\infty) + \rho g\beta_c(C(y,\tau) - C_\infty) - \varphi B_0^2 u(y,\tau) \quad (1)$$

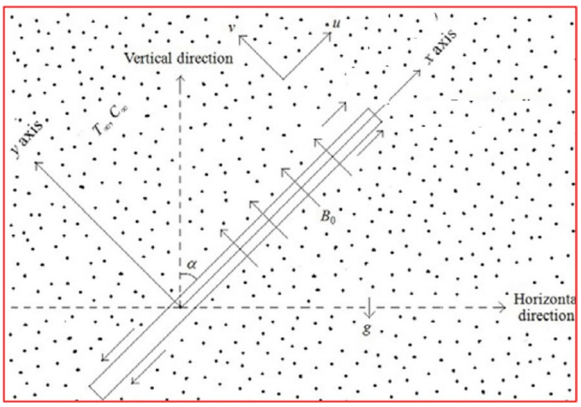

Fig. 1 Flow configuration of problem

$$\rho c_p \frac{\partial \theta(y,\tau)}{\partial \tau} = K \frac{\partial^2 \theta(y,\tau)}{\partial y^2} + Q_0(\theta(y,\tau) - \theta_\infty) \quad (2)$$

$$\frac{\partial C(y,\tau)}{\partial \tau} = D \frac{\partial^2 C(y,\tau)}{\partial y^2} - K_1(C(y,\tau) - C_\infty) \quad (3)$$

Justifying:

$$\left.\begin{aligned} &u(y,0) = 0, \qquad \theta(y,0) = \theta_\infty,\ C(y,0) = C_\infty, \\ &u(0,\tau) = A\tau^2, \qquad \theta(0,\tau) = \theta_w,\ \ C(0,\tau) = C_w, \\ &u(\infty,\tau) = 0, \qquad \theta(\infty,\tau) = \theta_\infty,\ C(\infty,\tau) = C_\infty. \end{aligned}\right\} \quad (4)$$

with μ (viscosity), k (thermal conductivity), g (gravity), Q_0 (heat generation), B_0 (magnetic field), β_c (concentration coefficient), β_θ (volumetric thermal expansion), $\theta(y,\tau)$, D (mass diffusivity), ρ (density), c_p (heat capacitance), and k_1 (reaction constant).

Intervening new variables [9]:

$$u^* = \frac{u}{(\nu^2 A)^{\frac{1}{5}}},\ y^* = \frac{yA^{\frac{1}{5}}}{\nu^{\frac{3}{5}}},\ \tau^* = \frac{\tau A^{\frac{2}{5}}}{\nu^{\frac{1}{5}}},$$
$$\theta^*(y,\tau) = \frac{\theta - \theta_\infty}{\theta_w - \theta_\infty},\ C^*(y,\tau) = \frac{C - C_\infty}{C_w - C_\infty}$$

Into Eqs. (1)–(4),

$$\frac{\partial u(y,\tau)}{\partial \tau} = \frac{\partial^2 u(y,\tau)}{\partial y^2} + Gr\theta(y,\tau) + GmC(y,\tau) - Hau(y,\tau) \quad (5)$$

$$\Pr \frac{\partial \theta(y,\tau)}{\partial \tau} = \frac{\partial^2 \theta(y,\tau)}{\partial y^2} + \delta \Pr \theta(y,\tau) \quad (6)$$

$$Sc \frac{\partial C(y,\tau)}{\partial \tau} = \frac{\partial^2 C(y,\tau)}{\partial y^2} - \omega Sc C(y,\tau) \quad (7)$$

$$\left.\begin{aligned} &u(y,0) = 0, \qquad \theta(y,0) = 0,\ C(y,0) = 0 \\ &u(0,\tau) = \tau^2, \qquad \theta(0,\tau) = 1,\ \ C(0,\tau) = 1 \\ &u(\infty,\tau) = 0, \qquad \theta(\infty,\tau) = 0,\ C(\infty,\tau) = 0 \end{aligned}\right\} \quad (8)$$

where $Gr = g\beta_\theta \Delta\theta A^{-\frac{3}{5}} \upsilon^{-\frac{1}{5}}$ is (thermal Grashof number), $\mathrm{Sc} = \frac{\upsilon}{D}$ (Schmidt constant), $Gm = g\beta_c \Delta C A^{-\frac{3}{5}} \upsilon^{-\frac{1}{5}}$ (mass Grashof constant), $\Pr = \frac{\mu c_p}{K}$ (Prandtl factor), $\delta = \frac{Q_0}{\rho c_p} A^{-\frac{2}{5}} \upsilon^{\frac{1}{5}}$ (heat generation), $\omega = k_1 A^{-\frac{2}{5}} \upsilon^{\frac{1}{5}}$ (reaction parameter), $H_a = \frac{\varphi}{\rho} B_0^2 A^{-\frac{2}{5}} \upsilon^{\frac{1}{5}}$ (Hartmann constant).

2.2 Entropy generation phenomenon

The creation of entropy generation is described by the following relations:

$$E_{gen} = \frac{K}{\theta_\infty^2}\left(\frac{\partial \theta}{\partial y}\right)^2 + \frac{D}{C_\infty^2}\left(\frac{\partial C}{\partial y}\right)^2 + \frac{\mu}{\theta_\infty}\left(\frac{\partial u}{\partial y}\right)^2 + \frac{\varphi B_0^2}{\theta_\infty} u^2 \quad (9)$$

Suggesting the new variables:

$\partial\theta/\partial y = \Delta\theta A^{\frac{1}{5}} \nu^{-\frac{3}{5}} \partial\theta^*/\partial y^*$

$\partial C/\partial y = \Delta C A^{\frac{1}{5}} \nu^{-\frac{3}{5}} \partial C^*/\partial y^*, \quad \partial u/\partial y = A^{\frac{2}{5}} \nu^{-\frac{1}{5}} \partial u^*/\partial y^*$

and added Eq. (9) leads to:

$$N_s = \left[\frac{D\zeta^2}{k\Omega^2}\left(\frac{\partial C}{\partial y}\right)^2 + \left(\frac{\partial \theta}{\partial y}\right)^2 + H_a \frac{B_r}{\Omega} u^2 + \frac{B_r}{\Omega}\left(\frac{\partial u}{\partial y}\right)^2\right] \quad (10)$$

where

$N_s = \frac{E_{gen} \nu^{\frac{6}{5}} \theta_\infty^2}{kA^{2/5}(\Delta\theta)^2},\ Br = \frac{\mu A^{\frac{2}{5}} \nu^{\frac{4}{5}}}{k\Delta\theta},\ \Omega = \frac{\Delta\theta}{\theta_\infty} = \frac{\theta_w - \theta_\infty}{\theta_\infty},$

$\zeta = \frac{\Delta C}{C_\infty} = \frac{C_w - C_\infty}{C_\infty}.$

2.3 Bejan numbers

The Bejan constant is important to present the prediction of entropy production and thermal saturation profile. The Bejan constant is expressed as:

$$BN = \frac{\frac{K}{\theta_\infty^2}\left(\frac{\partial \theta}{\partial y}\right)^2}{\frac{K}{\theta_\infty^2}\left(\frac{\partial \theta}{\partial y}\right)^2 + \frac{D}{C_\infty^2}\left(\frac{\partial C}{\partial y}\right)^2 + \frac{\mu}{\theta_\infty}\left(\frac{\partial u}{\partial y}\right)^2 + \frac{\varphi B_0^2}{\theta_\infty} u^2} \quad (11)$$

and

$$BN = \frac{\left(\frac{\partial \theta}{\partial \eta}\right)^2}{\left(\frac{\partial \theta}{\partial y}\right)^2 + \frac{D\zeta^2}{k\Omega^2}\left(\frac{\partial C}{\partial y}\right)^2 + \frac{B_r}{\Omega}\left(\frac{\partial u}{\partial y}\right)^2 + H_a \frac{B_r}{\Omega} u^2} \quad (12)$$

2.4 Implementation of Laplace transform scheme

The assessment via Laplace transform is essentially evaluated for Eqs. (5)–(8). Utilizing the Laplace operator as:

$$q\,\bar{u}(y,q) = \frac{\partial^2 \bar{u}(\eta,q)}{\partial y^2} + Gr\,\bar{\theta}(y,q) + Gm\,\bar{C}(y,q) - H_a \bar{u}(y,q) \quad (13)$$

$$\bar{u}(0,q) = \frac{2}{q^3}, \quad \bar{u}(\infty,q) = 0 \quad (14)$$

$$\Pr q\bar{\theta}(y,q) = \frac{\partial^2 \bar{\theta}(y,q)}{\partial y^2} + \delta \Pr \bar{\theta}(y,q) \quad (15)$$

$$\overline{\theta}(0,q)=\frac{1}{q},\quad \overline{\theta}(\infty,q)=0 \tag{16}$$

$$Sc\,q\overline{C}(y,q)=\frac{\partial^2\overline{C}(y,q)}{\partial y^2}-Sc\,\omega\overline{C}(y,q) \tag{17}$$

$$\overline{C}(0,q)=\frac{1}{q},\quad \overline{C}(\infty,q)=0 \tag{18}$$

The resulted solution is:

$$\overline{\theta}(y,q)=\frac{e^{-y\sqrt{(q-\delta)\,\mathrm{Pr}}}}{q} \tag{19}$$

$$\theta(y,\tau)=\frac{1}{2}\left[e^{-y\sqrt{-\delta\,\mathrm{Pr}}}erfc\left(\frac{y\sqrt{\mathrm{Pr}}}{2\sqrt{\tau}}-\sqrt{-\delta\,\mathrm{Pr}\,t}\right)+e^{y\sqrt{-\delta\,\mathrm{Pr}}}erfc\left(\frac{y\sqrt{\mathrm{Pr}}}{2\sqrt{\tau}}+\sqrt{-\delta\,\mathrm{Pr}\,t}\right)\right] \tag{20}$$

$$\overline{C}(y,q)=\frac{e^{-y\sqrt{(q+\omega)Sc}}}{q} \tag{21}$$

which leads to:

$$C(y,\tau)=\frac{1}{2}\left[e^{-y\sqrt{\omega Sc}}erfc\left(\frac{y\sqrt{Sc}}{2\sqrt{\tau}}-\sqrt{\omega Sct}\right)+e^{y\sqrt{\omega Sc}}erfc\left(\frac{y\sqrt{Sc}}{2\sqrt{\tau}}+\sqrt{\omega Sct}\right)\right] \tag{22}$$

Equation (13) leads to:

$$\bar{u}(y,q)=\frac{2}{q^3}e^{-y\sqrt{H_a+q}}+\frac{1}{a_0}\frac{1}{q-A}e^{-y\sqrt{H_a+q}}-\frac{1}{a_0}\frac{1}{q}e^{-y\sqrt{H_a+q}}-\frac{1}{b_0}\frac{1}{q+B}e^{-y\sqrt{H_a+q}}+\frac{1}{b_0}\frac{1}{q}e^{-y\sqrt{H_a+q}}-\frac{1}{a_0}\frac{1}{q-A}e^{-y\sqrt{\mathrm{Pr}}\sqrt{q-\delta}}+\frac{1}{a_0}\frac{1}{q}e^{-y\sqrt{\mathrm{Pr}}\sqrt{q-\delta}}+\frac{1}{b_0}\frac{1}{q+B}e^{-y\sqrt{Sc}\sqrt{q+\omega}}-\frac{1}{b_0}\frac{1}{q}e^{-y\sqrt{Sc}\sqrt{q+\omega}} \tag{23}$$

as.

$a_0=\frac{\delta\ \mathrm{Pr}+\mathrm{H}_a}{Gr}$, $a_1=\frac{\mathrm{Pr}\text{ - }1}{Gr}$, $b_0=\frac{\omega\ \mathrm{Sc}\text{ - }\mathrm{H}_a}{Gm}$, $\mathrm{b}_1=\frac{\mathrm{Sc}\text{ - }1}{Gm}$, $\mathrm{A}=\frac{a_0}{a_1}$, $\mathrm{B}=\frac{b_0}{b_1}$.

Implementing the Laplace operator as,

$$u(y,\tau)=u_1(y,\tau)+y_2(y,\tau)+u_3(y,\tau)+u_4(y,\tau) \tag{24}$$

$$u_1(y,\tau)=2\left[e^{-y\sqrt{H_a}}erfc\left(\frac{y}{2\sqrt{\tau}}-\sqrt{H_a\tau}\right)\frac{1}{4}\left(\tau^2-\frac{y}{4\sqrt{H_a}}\right)-e^{y\sqrt{H_a}}erfc\left(\frac{y}{2\sqrt{\tau}}+\sqrt{H_a\tau}\right)\frac{1}{4}\left(\tau^2+\frac{y}{4\sqrt{H_a}}\right)\right]+\frac{1}{2a_0}e^{A\tau}\left[e^{-y\sqrt{H_a+A}}erfc\left(\frac{y}{2\sqrt{\tau}}-\sqrt{(H_a+A)\tau}\right)+e^{y\sqrt{H_a+A}}erfc\left(\frac{y}{2\sqrt{\tau}}+\sqrt{(H_a+A)\tau}\right)\right] \tag{25}$$

$$u_2(y,\tau)=\frac{1}{2}\left(\frac{1}{b_0}-\frac{1}{a_0}\right)\left[e^{-y\sqrt{H_a}}erfc\left(\frac{y}{2\sqrt{\tau}}-\sqrt{H_a\tau}\right)+e^{y\sqrt{H_a}}erfc\left(\frac{y}{2\sqrt{\tau}}+\sqrt{H_a\tau}\right)\right]-\frac{1}{2b_0}e^{-B\tau}\left[e^{-y\sqrt{H_a-B}}erfc\left(\frac{y}{2\sqrt{\tau}}-\sqrt{(H_a-B)\tau}\right)+e^{y\sqrt{H_a-B}}erfc\left(\frac{y}{2\sqrt{\tau}}+\sqrt{(H_a-B)\tau}\right)\right] \tag{26}$$

$$u_3(y,\tau)=-\frac{1}{2a_0}e^{A\tau}\left(e^{-y\sqrt{\mathrm{Pr}(A-\delta)}}erfc\left(\frac{y\sqrt{\mathrm{Pr}}}{2\sqrt{\tau}}-\sqrt{(A-\delta)\tau}\right)+e^{y\sqrt{\mathrm{Pr}(A-\delta)}}erfc\left(\frac{y\sqrt{\mathrm{Pr}}}{2\sqrt{\tau}}+\sqrt{(A-\delta)\tau}\right)\right)+\frac{1}{2a_0}\left(e^{-y\sqrt{-\delta\,\mathrm{Pr}}}erfc\left(\frac{y\sqrt{\mathrm{Pr}}}{2\sqrt{\tau}}-\sqrt{-\delta\tau}\right)+e^{y\sqrt{-\delta\,\mathrm{Pr}}}erfc\left(\frac{y\sqrt{\mathrm{Pr}}}{2\sqrt{\tau}}+\sqrt{-\delta\tau}\right)\right) \tag{27}$$

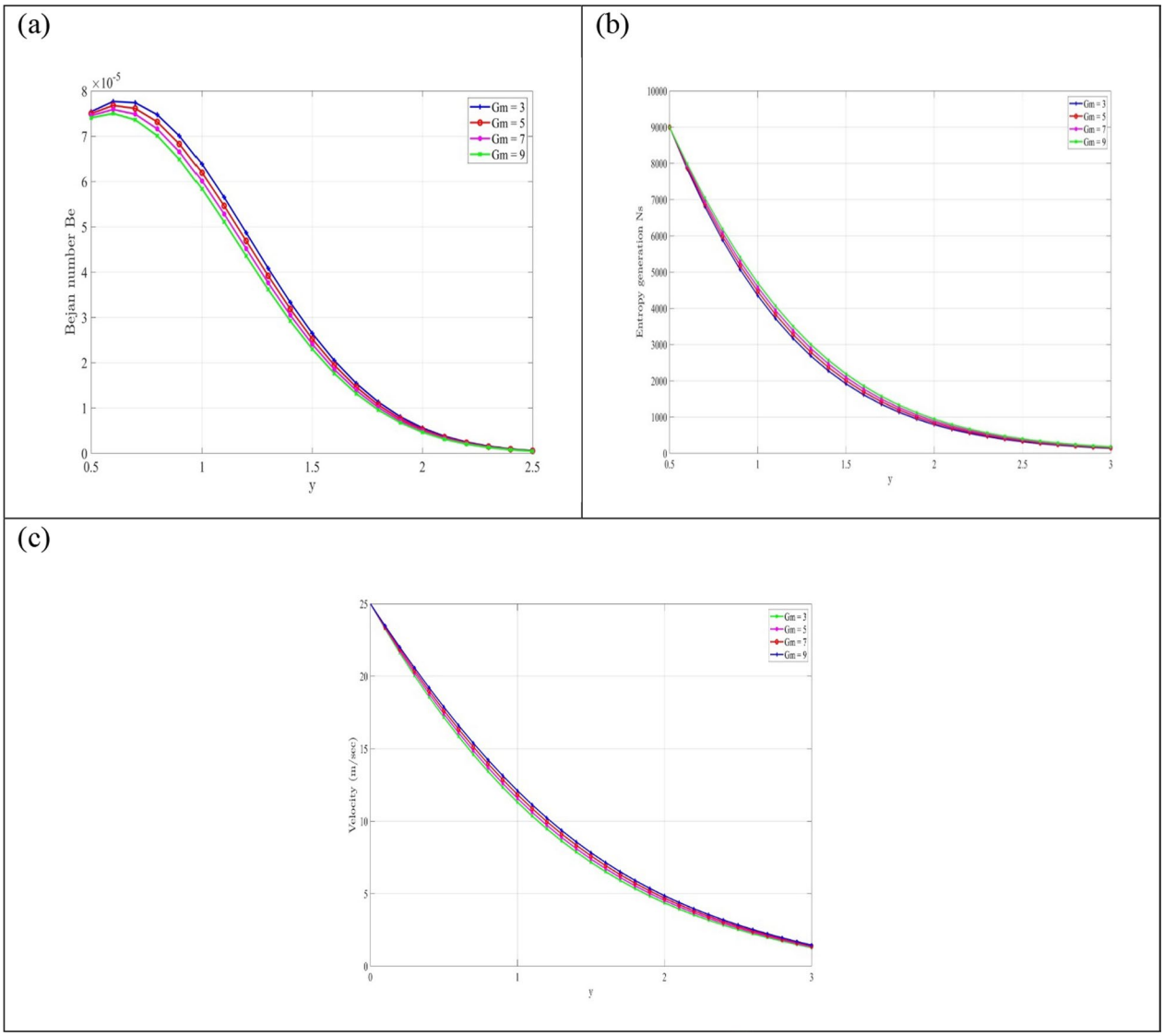

Fig. 2 **a–c**: Assessment of Bejan number against Gm, **b** assessment of entropy phenomenon against Gm, and **c** assessment of velocity against Gm.

$$u_4(y,\tau) = \frac{1}{2b_0}e^{-B\tau}\left(e^{-y\sqrt{Sc(\omega-B)}}erfc\left(\frac{y\sqrt{Sc}}{2\sqrt{\tau}} - \sqrt{(\omega-B)\tau}\right) + e^{y\sqrt{Sc(\omega-B)}}erfc\left(\frac{y\sqrt{Sc}}{2\sqrt{\tau}} + \sqrt{(\omega-B)\tau}\right)\right) - \frac{1}{2b_0}\left(e^{-y\sqrt{\omega Sc}}erfc\left(\frac{y\sqrt{Sc}}{2\sqrt{\tau}} - \sqrt{\omega\tau}\right) + e^{y\sqrt{\omega Sc}}erfc\left(\frac{y\sqrt{Sc}}{2\sqrt{\tau}} + \sqrt{\omega\tau}\right)\right) \tag{28}$$

Defining the wall drag force:

$$c_f = \left.\frac{\partial v(y,\tau)}{\partial y}\right|_{y=0} \tag{29}$$

Now defining the Nusselt quantity as:

$$Nu = \left.\frac{\partial \theta(y,\tau)}{\partial y}\right|_{y=0} \tag{30}$$

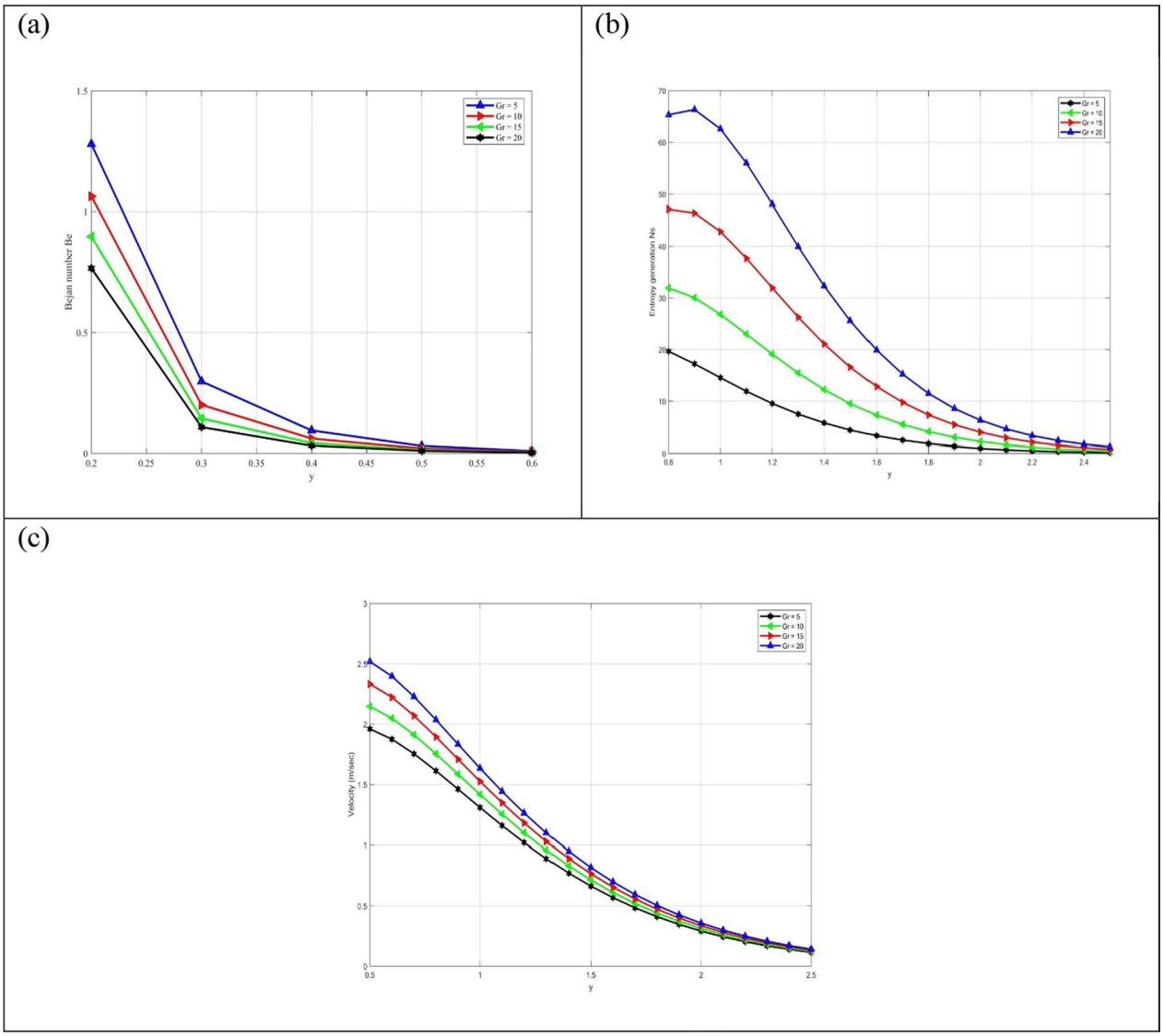

Fig. 3 **a–c**: Assessment of Bejan number for Gr, **b** assessment of entropy generation for *Gr*, **c** assessment of velocity profile for Gr.

3 Results

The optimized thermal phenomenon for mixed convection problem has been discussed. The modeled problem is supported with the perturbation technique. In the current section, graphical outcomes are presented in view of different parameters. Figure 2a compromises the observations for Bejan number *BN* under the impact of mass Grashof number Gm. The decreasing observations are listed for Bejan number when peak changes have been assigned to Gm. Physically, Grashof number presents a special attention in the mass and heat transfer phenomenon. It associated the relation between buoyancy force and viscous force in the thermal transport phenomenon. The declining change in *BN* due to Gm shows that viscous forces play dominant role in controlling the optimized phenomenon. Figure 2b shows the entropy generation N_s against increasing Gm. A boosted impact in N_s for Gm have been results. On this end, it is concluded that the mixed convection phenomenon is important for enhancing

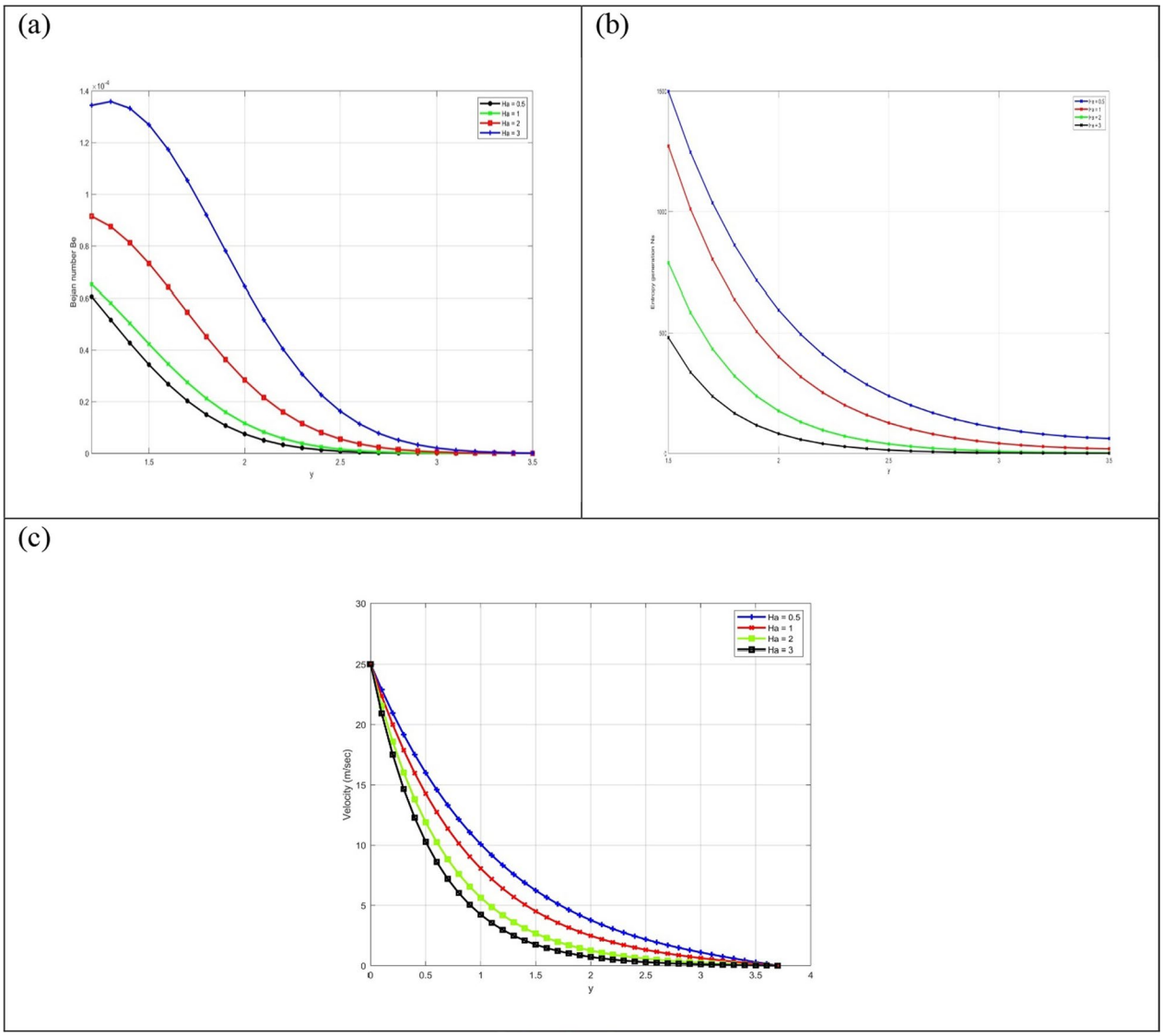

Fig. 4 **a–c**: **a** Assessment of Bejan number for *Ha*, **b** assessment of entropy generation for *Ha*, **c** assessment of velocity profile *Ha*

the optimized outcomes. Figure 2c deduces the results for changing velocity for Gm.. An increment in velocity is noticed when *Gm* is enhanced. Figure 3a–c reports the onset of thermal Grashof number Gr to report the change in entropy generation N_s, velocity profile and Bejan number BN. The reducing change in BN with large Gr is resulted in Fig. 3a. Figure 3b discloses the assistance of Gr on entropy generation N_s. With larger change assigning to Gr, the entropy phenomenon boosted. The same results discussed for velocity are noticed in Fig. 3c. Figure 4a pronounces the insight of Bejan number via Hartmann constant Ha. An enlarge change is noticed under the larger assigning values of Ha. The enhanced trend in Bejan number is claimed in Fig. 4b. Such outcomes are associated with the Lorentz force. Some results are noted for entropy generation in view of Ha. However, a contracted behavior is observed for velocity in Fig. 4c. Figure 5a–c announces the change in Bejan number with larger variation of Schmidt number Sc on BN, N_s and velocity. The

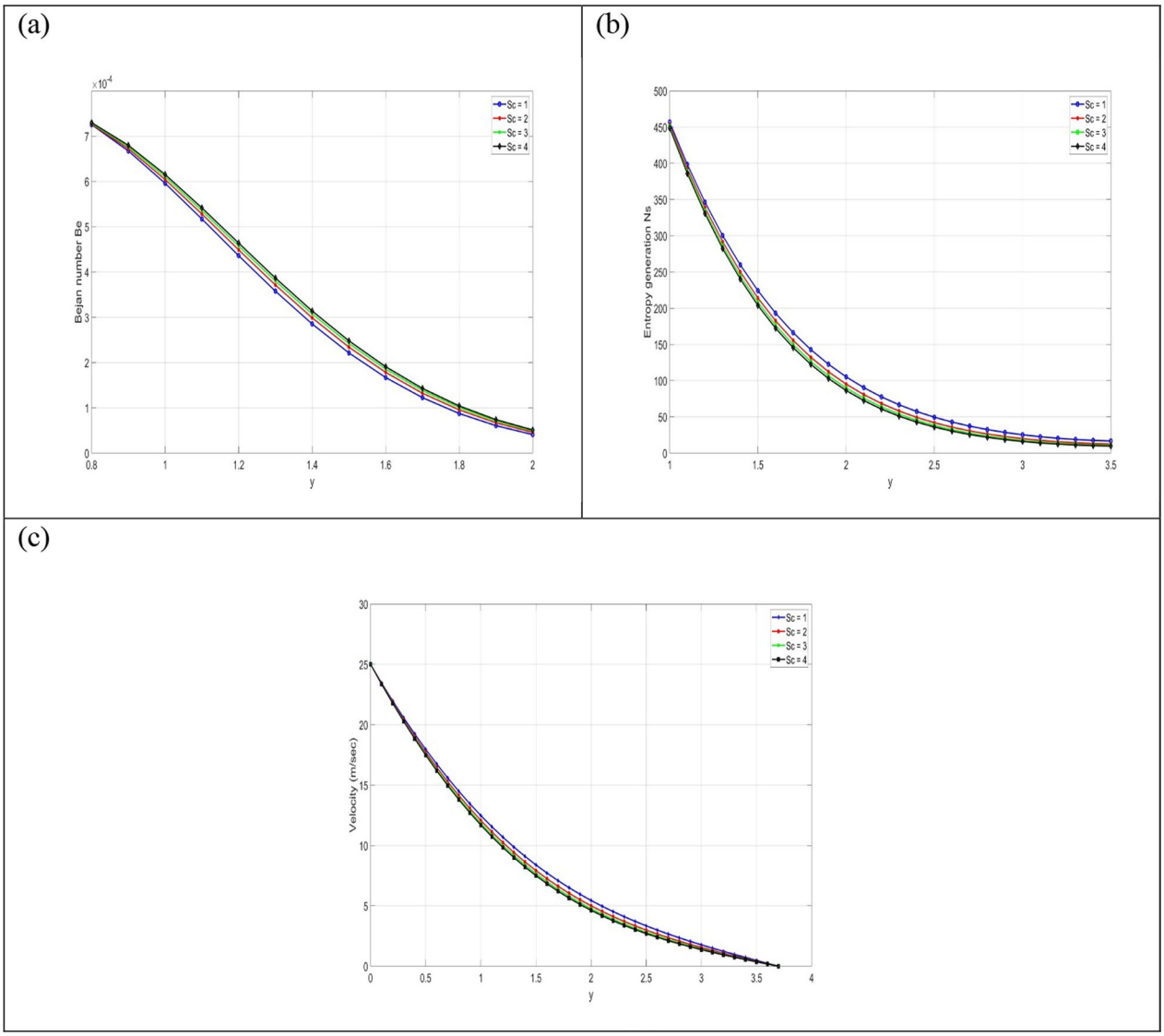

Fig. 5 **a–c**: **a** Assessment of Bejan number for *Sc*, **b** assessment of entropy phenomenon for *Sc* **c** assessment of velocity profile for *Sc*.

increasing impact of *Sc* on Bejan number while less observations for entropy generation field is resulted. The control of velocity is predicted for Schmidt number. Such features are noted due to low mass diffusivity. Figure 6 reports the variation of skin friction due to distinct values of *Gr*. It has been noticed that skin friction reduces due to *Gr*. Figure 7 explains the assessment for Nusselt number with different values of Schmidt number *Sc*. Low Nusselt number profile is predicted due to *Sc*. These outcomes are associated with the low mass diffusivity.

Table 1 shows the attribution of Bejan number, wall shear and entropy generation in view of Hartmann number and Schmidt number. A leading role of both parameters beyond the variation of Bejan number has been observed. However, less observations are claimed for entropy generation and Bejan number. Table 2 analyzes the significance of Grashof number *Gr* on velocity, Bejan number, Nusselt number and wall shear force. The analysis is performed for fixed numerical values of *Ha* and time *t*. The lower observations for Bejan number

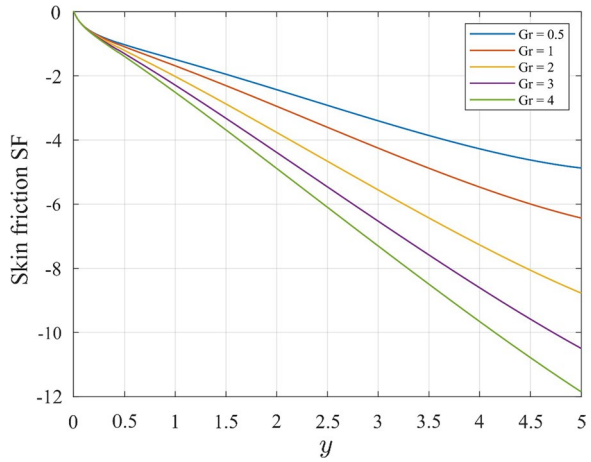

Fig. 6 Analysis for skin friction with variation of Gr.

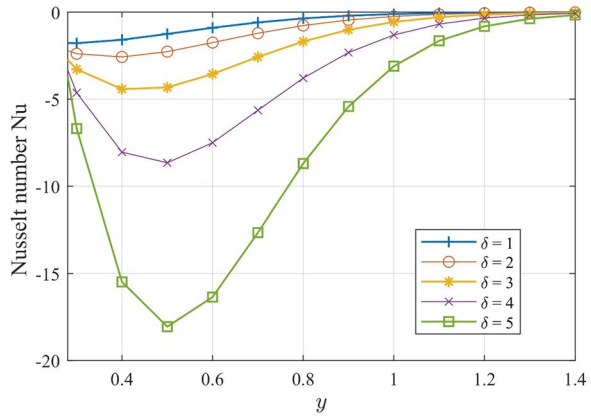

Fig. 7 Analysis for Nusselt number with variation of δ.

due to variation of *Gr* have been inspected. However, the velocity field and entropy generation increase against the larger variation of *Gr*. Moreover, a decrement in wall shear is also noticed due to *Gr*. A decrement in optimized phenomenon and velocity in view of mass and thermal Grashof numbers have been disclosed which are represented in Tables 3 and 4. From Table 4, Bejan number decreases for temperature difference constant.

4 Conclusion

The heat and mass transfer phenomenon for mixed convection flow with entropy generation impact via flat plate is discussed under the influence of external heat source and chemical reaction. The solution technique is adopted with Laplace technique. The association of parameters with Bejan number, velocity and entropy generation is discussed, summarizing main observations as follows:

- By enhancing both heat and mass Grashof numbers, a control of entropy generation phenomenon is noticed.
- The contribution of magnetic force boosted the entropy generation.
- Upon increasing mass Grashof number, the Bejan number declined
- The enhancing lower change in entropy assessment and Bejan profile is noted due to Schmidt number, respectively.
- The velocity field increased for mass Grashof constant as well as thermal Grashof number.
- The decreasing numerical values of Bejan profile and entropy generation are being observed for Hartmann constant and Schmidt number.
- These results can be further updated by utilizing the bioconvection applications and artificial neural network. Moreover, the geometry of the proposed equations will be investigated in addition to numerical investigations will involve different types of fractional differential operators will be studied.

Table 1 FDM simulations for *Ha*

Ha	*t*	Gr	*y*	*u*	BN	Ns	SF
0.08	2	0.05	0.5	0.7045	0.0101	3.5887	−0.3519
0.5	2	0.05	0.5	0.6554	0.0108	3.4244	−0.3192
0.8	2	0.05	0.5	0.6240	0.0116	3.2444	−0.2984
1	2	0.05	0.5	0.6046	0.0123	3.1100	−0.2855
2	2	0.05	0.5	0.5221	0.0165	2.4115	−0.2315
3	2	0.05	0.5	0.4580	0.0228	1.8150	−0.1908
4	2	0.05	0.5	0.4069	0.0315	1.3611	−0.1593

Table 2 FDM simulations for v Gr

Gr	Ha	*t*	*y*	*u*	BN	Ns	SF
0.08	0.5	2	0.5	0.6713	0.0105	3.5619	−0.3259
0.5	0.5	2	0.5	0.8933	0.0067	5.7749	−0.4190
0.8	0.5	2	0.5	1.0519	0.0051	7.6841	−0.4856
1	0.5	2	0.5	1.1576	0.0044	9.1091	−0.5299
2	0.5	2	0.5	1.6862	0.0023	18.0597	−0.7517
3	0.5	2	0.5	2.2148	0.0014	30.0531	−0.9735
4	0.5	2	0.5	2.7435	9.3651×10^{-4}	45.0892	−1.1952

Table 3 FDM simulations for *Gm*

Gm	*t*	Gr	Ha	*y*	*u*	BN	Ns	SF
0.08	2	0.05	0.5	0.5	0.3875	0.0510	0.7882	−0.1566
0.5	2	0.05	0.5	0.5	0.4104	0.0422	0.9405	−0.1705
0.8	2	0.05	0.5	0.5	0.4267	0.0372	1.0576	−0.1804
1	2	0.05	0.5	0.5	0.4376	0.0343	1.1396	−0.1870
2	2	0.05	0.5	0.5	0.4920	0.0241	1.5953	−0.2201
3	2	0.05	0.5	0.5	0.5465	0.0178	2.1280	−0.2531
5	2	0.05	0.5	0.5	0.6554	0.0108	3.4244	−0.3192

Table 4 FDM simulations for Ω

Ω	*t*	Gr	Ha	*y*	Bejan number	Nusselt number
0.08	2	0.05	0.5	0.5	0.0015	24.0831
0.5	2	0.05	0.5	0.5	0.0096	3.8533
1	2	0.05	0.5	0.5	0.0192	1.9266
2	2	0.05	0.5	0.5	0.0384	0.9633
3	2	0.05	0.5	0.5	0.0577	0.6422
4	2	0.05	0.5	0.5	0.0769	0.4817
5	2	0.05	0.5	0.5	0.0961	0.3853

List of symbols

u Velocity of the fluid (ms^{-1})
θ Temperature of the fluid (K)
C Concentration of the fluid
g Acceleration due to gravity (ms^{-2})
c_p Specific heat at a constant pressure (j kg^{-1} K^{-1})
Gr Thermal Grashof number k
k Thermal conductivity of the fluid (W m^{-2} K^{-1})
Gm The mass Grashof number
Sc The Schmidt number
ω The chemical reaction parameter
Nu Nusselt number
Pr Prandtl number
θ_∞ Fluid temperature far away from the plate (K)
q Laplace transforms parameter
K Porosity parameter
D The mass diffusivity
k_1 The chemical reaction parameter
Q_0 The heat generation term
δ The heat generation parameter
A Random constant (ms^{-2})

Greek symbols

ν Kinematic viscosity of the fluid (m^2s^1)
μ Dynamic viscosity (kg m^1s^{-1})
ρ Fluid density (kg ms^3)
β_θ The volumetric coefficient of thermal expansion (K^1)
β The Casson fluid parameter
β_c The coefficient of concentration
Br The Brinkman number
Ω The dimensionless temperature function

Acknowledgements
The author extends the appreciation to the Deanship of Postgraduate Studies and Scientific Research at Majmaah University for funding this research work through the project number R-2024-1053.

Author contributions
Abdelhameed worked alone in editing, writing, review (single work).

Funding
This work was supported by the Majmaah University (Grant No. R-2024-1053).

Availability of data and materials
All data are available in the manuscript.

Declarations

Ethics approval and consent to participate
Not applicable.

Consent for publication
Not applicable.

Competing interests
We declare here that the manuscript has no competing interest.

Received: 5 September 2023 Accepted: 17 April 2024
Published online: 25 April 2024

References

1. Basak T, Roy S, Sharma PK, Pop I (2009) Analysis of mixed convection flows within a square cavity with uniform and non-uniform heating of bottom wall. Int J Therm Sci 48(5):891–912
2. Khanafer K, Aithal SM (2013) Laminar mixed convection flow and heat transfer characteristics in a lid driven cavity with a circular cylinder. Int J Heat Mass Transfer 66:200–209
3. Huang TM, Chie G, Win A (1995) Mixed convection flow and heat transfer in a heated vertical convergent channel. Int J Heat and Mass Transfer 38(13):2445–2456
4. Maughan JR, Incropera FP (1987) Experiments on mixed convection heat transfer for airflow in a horizontal and inclined channel. Int J Heat Mass Transfer 30(7):1307–1318
5. Ahmed SE, Zehba R, Arafa AAM, Hussein SA (2023) FEM treatments for MHD highly mixed convection flow within partially heated double-lid driven odd-shaped enclosures using ternary composition nanofluids. Int Commun Heat Mass Transfer 145:106854
6. Rehman MIU, Chen H, Hamid A, Qi H (2023) Numerical analysis of unsteady non-linear mixed convection flow of reiner-philippoff nanofluid along Falkner-Skan wedge with new mass flux condition. Chem Phys Lett 830:140799
7. Hayat T, Razaq A, Khan SA, Momani S (2023) Soret and Dufour impacts in entropy optimized mixed convective flow. Int Commun Heat Mass Transfer 141:106575
8. Sharma BK, Khanduri U, Mishra NK, Mekheimer KS (2023) Combined effect of thermophoresis and Brownian motion on MHD mixed convective flow over an inclined stretching surface with radiation and chemical reaction. Int J Modern Phys B 37(10):2350095
9. Chen TS, Moutsoglou A, Armaly BF (1982) Thermal instability of mixed convection flow over inclined surfaces. Numer Heat Transf, Part A Appl 5(3):343–352
10. Ige EO, Falodun BO, Adebiyi DO, Khan SU (2023) Computational analysis of mixed convection in a blood-based hybrid nanoliquid under boussinesq approximation in a transient regime. J Comput Biophys Chem 22(03):347–359
11. Saeed ST, Riaz MB, Baleanu D (2021) A fractional study of generalized Oldroyd-B fluid with ramped conditions via local & non-local kernels. Nonlinear Eng 10(1):177–186
12. Rehman AU, Riaz MB, Akgül A, Saeed ST, Baleanu D (2021) Heat and mass transport impact on MHD second-grade fluid: a comparative analysis of fractional operators. Heat Transfer 50(7):7042–7064
13. Saeed ST, Riaz MB, Awrejcewicz J, Ahmad H (2021) Exact symmetric solutions of MHD casson fluid using chemically reactive flow with generalized boundary conditions. Energies 14(19):6243
14. A. Bejan, (1979) "A study of entropy generation in fundamental convective heat transfer.
15. Li S, Khan MI, Alruqi AB, Khan SU, Abdullaev SS, Fadhl BM, Makhdoum BM (2023) Entropy optimized flow of Sutterby nanomaterial subject to porous medium: Buongiorno nanofluid model. Heliyon 9(7):e17784
16. Abdelhameed TN (2022) Entropy generation of MHD flow of sodium alginate (C6H9NAO7) fluid in thermal engineering. Sci Rep 12:701. https://doi.org/10.1038/s41598-021-04655-0
17. Shah Z, Jafaryar M, Sheikholeslami M, Ikramullah, Kumam P (2021) Heat transfer intensification of nanomaterial with involve of swirl flow device concerning entropy generation. Sci Rep 11(1):12504
18. Wang F, Khan SA, Gouadria S, El-Zahar ER, Khan MI, Khan SU, Li YM (2022) Entropy optimized flow of Darcy-Forchheimer viscous fluid with cubic autocatalysis chemical reactions. Int J Hydrogen Energy 47(5):13911–13920
19. Alsallami SA, Usman K, SU., Ghaffari, A., Khan, M. I., El-Shorbagy, M. A., & Khan, M. R. (2022) Numerical simulations for optimised flow of second-grade nanofluid due to rotating disk with nonlinear thermal radiation: Chebyshev spectral collocation method analysis. Pramana 96(2):98
20. Turkyilmazoglu M (2020) Velocity slip and entropy generation phenomena in thermal transport through metallic porous channel. J Non-Equilib Thermodyn 45(3):247–256
21. Batool S, Al-Khaled K, Abbas T, Hassan QMU, Khan KA, Ghachem K, Kolsi L (2023) Double diffusion Forchheimer flow of Carreau-Yasuda nanofluid with bioconvection and entropy generation: Thermal optimized analysis via non-Fourier model. Case Stud Therm Eng 48:103172
22. Liu M, Li S, Zhengren Wu, Zhang K, Wang S, Liang X (2019) Entropy generation analysis for grooved structure plate flow. Eur J Mech-B/Fluids 77:87–97
23. Iftikhar B, Javed T, Siddiqu MA (2023) Entropy generation analysis during MHD mixed convection flow of non-Newtonian fluid saturated inside the square cavity. J Comput Sci 66:101907
24. Sheikholeslami M (2019) New computational approach for exergy and entropy analysis of nanofluid under the impact of Lorentz force through a porous media. Comput Methods Appl Mech Eng 344:319–333
25. Sheikholeslami M (2019) Numerical approach for MHD Al2O3-water nanofluid transportation inside a permeable medium using innovative computer method. Comput Methods Appl Mech Eng 344:306–318
26. Sheikholeslami M (2023) Numerical investigation for concentrated photovoltaic solar system in existence of paraffin equipped with MWCNT nanoparticles. Sustain Cities Soc 99:104901
27. Sheikholeslami M, Khalili Z (2024) Simulation for impact of nanofluid spectral splitter on efficiency of concentrated solar photovoltaic thermal system. Sustain Cities Soc 101:105139
28. Sheikholeslami M, Khalili Z, Scardi P, Ataollahi N (2023) Concentrated solar photovoltaic cell equipped with thermoelectric layer in presence of nanofluid flow within porous heat sink: impact of dust accumulation. Sustain Cities Soc 98:104866

Publisher's Note